Available online at www.sciencedirect.com
ScienceDirect
Polymer 49 (2008) 579–587
polymer
www.elsevier.com/locate/polymer

Dendritic crystallization in thin films of PEO/PMMA blends: A comparison to crystallization in small molecule liquids ☆

Brian C. Okerberg [a,*], Hervé Marand [b], Jack F. Douglas [c]

[a] Department of Materials Science and Engineering, Virginia Tech, Blacksburg, VA 24061, United States
[b] Department of Chemistry, Davidson Hall, Virginia Tech, Blacksburg, VA 24061, United States
[c] Polymers Division, National Institute of Standards and Technology, Gaithersburg, MD 20899, United States

Received 28 September 2007; received in revised form 14 November 2007; accepted 18 November 2007
Available online 21 November 2007

Abstract

Dendritic crystallization of poly(ethylene oxide) (PEO)/poly(methyl methacrylate) (PMMA) thin films is reported. The film thickness is kept constant while the PMMA molar mass and blend composition are varied. Some basic features of dendritic growth, such as the diffusion length and tip curvature are discussed. The diffusion coefficient is tuned by varying the molar mass of the non-crystallizable PMMA and the blend composition. The observed dendrite tip radius is on the order of 50 nm and the shape of the growth envelope varies from square to needle-like as the PMMA molar mass or PMMA content is increased. The sidebranch spacing increases with the distance from the dendrite trunk with a power-law relationship that is also dependent on the PMMA molar mass and PMMA content. This coarsening process is similar to that reported for other classes of materials. These similarities (the curved dendrite tip, power-law relationship of the sidebranches, and the sidebranch coarsening processes) indicate that the large scale crystallization morphologies of the polymeric materials we study are similar to those found in crystallization of small molecules and metals.

Keywords: Crystallization; Thin films; Blends

1. Introduction

Dendritic solidification has been studied well for over a century and in recent years an understanding of this growth process has emerged for small molecules and metals through the interplay of both measurements [1–15] and theoretical modeling [16–19]. Interest in dendritic growth stems from its importance in the properties of polycrystalline materials and the fascinating variety of patterns formed during crystallization. Traditional studies on dendritic growth have focused on small molecules and metals because of the prevalence of dendritic morphologies in these materials. A number of good reviews on dendritic growth in metals and small molecules have recently been published [20–23]. The present work explores the similarities of this growth phenomenon to dendritic growth observed during polymer crystallization.

Diffusion of heat or solute away from the growth front is an important aspect of the dendritic growth process. When the thermodynamic driving force for crystallization becomes strong or impurities are added to the system, the crystallization front becomes unstable, and flat interfaces and regular crystal patterns give way to crystallization patterns that are characterized by dendritic branching. Anisotropy in either the surface free energy of the crystal or the kinetics of molecular attachment promotes dendritic growth. Characterization of the dendritic morphology often involves measurements of the crystal growth velocity, tip radius, sidebranch spacing, and sidebranch amplitude. These quantities contain information about the

☆ Official contribution of the National Institute of Standards and Technology; not subject to copyright in the United States.

* Corresponding author. Present address: Polymers Division, National Institute of Standards and Technology, Stop 8541, Gaithersburg, MD 20899, United States. Tel.: +1 301 975 5230.
E-mail addresses: bokerber@vt.edu, brian.okerberg@nist.gov (B.C. Okerberg).

0032-3861/$ - see front matter © 2008 Elsevier Ltd. All rights reserved.
doi:10.1016/j.polymer.2007.11.034

underlying physics of dendritic growth and allow for comparisons of experimental observations with theoretical models [13].

Symmetric dendrites are not a universal pattern of crystallization. For example, bulk polymeric materials usually crystallize in the form of spherulites, which are spherically symmetric polycrystalline growth structures characterized by extensive non-crystallographic branching. Small molecule fluids also form spherulitic structures exhibiting a similar geometry if crystallization occurs in the presence of a substantial number of impurities or if the crystallization occurs at high supercooling [24–26] where dynamic heterogeneities are known to be present in the fluid [27,28].

Early studies on crystallization of polyethylene from solution by Keller [29], Khoury and Padden [30], Geil and Reneker [31], and Wunderlich and Sullivan [32] indicated that dendritic crystallization could also occur in polymeric materials under certain conditions, such as crystallization from solution. However, this type of growth has not been a focus of much research since symmetric dendritic growth is not characteristic of polymeric materials in the bulk. Dendritic growth with apparent crystallographic branching has recently been reported for a number of melt-crystallized polymers in ultrathin films, including polyethylene (PE) [33], isotactic polystyrene (iPS) [34–36], poly(ethylene oxide) (PEO) [37], poly(caprolactone) [38,39], poly-2-vinylpyridine–poly(ethylene oxide) (P2VP–PEO) block copolymers [40], and poly(ethylene oxide) (PEO)/poly(methyl methacrylate) (PMMA) blends [41–43]. These studies have stressed the importance of diffusion fields surrounding the crystal, as well as changes in the anisotropy with supercooling [44]. The mechanisms that engender this type of crystallization morphology in ultrathin polymers remain unclear, however, more studies on crystallization in thin films are clearly needed.

In this regard, Ferreiro and coworkers studied dendritic crystallization in blends of PEO/PMMA where the addition of amorphous PMMA allowed for the 'tuning' of the crystallization morphology. With increasing PMMA content, the spherulitic morphology transformed into a symmetric dendritic morphology, an effect that Ferreiro and coworkers attribute to a progressive change in the surface tension anisotropy with dilution of PEO by PMMA. Ferreiro and coworkers also made one of the first attempts to compare dendritic growth morphologies in polymeric melts with those observed in metals by comparing the crystallization patterns of PEO/PMMA blends with those observed in phase-field simulations of Ni/Cu alloys [41,42]. In these simulations, the effective surface tension anisotropy was varied resulting in a variety of morphologies, ranging from the dense-branched morphology (DBM) to dendrites. Early work on blends of liquid crystal molecules [45] claimed to achieve a similar effect of varying the surface tension anisotropy and the morphology, but the effects were less dramatic.

Despite these comparisons between polymeric materials and small molecules, many aspects of dendrite formation in polymeric materials remain unclear. Specifically, what are the conditions under which the faceted growth patterns transform into symmetric dendrites? Do these patterns develop by the same mechanisms as the ones proposed for other materials? Are sidebranch formation and the associated coarsening processes also similar?

Studies on pattern formation in polymeric materials may also offer new insights into crystallization in a broader context since it is often easier to study the growth processes in these systems due to their much slower nature and the availability of measurement techniques (such as atomic force microscopy) that exploit the capacity to vitrify polymeric materials. In addition, these materials offer unique possibilities for testing theory. For example, by varying the polymer molar mass, the diffusion coefficient can change significantly while the crystal growth velocity remains relatively constant. In small molecule systems, similar changes in the diffusion coefficient would require the use of a different solvent which can lead to changes in a number of experimental parameters. For example, Akamatsu et al. attempted to vary the diffusion coefficient in liquid-expanded/liquid-condensed phase transitions of 2D systems by varying the viscosity of the liquid sublayer, but reported problems with interpretation of the results due to complexities related to 'hydrodynamic coupling' [46]. Polymer mixtures are a natural choice for these studies since the molar mass of the amorphous component can be used as a direct means of controlling the diffusion coefficient.

In the current study, we focus on the dendritic regions of growth identified in our morphological map for crystallization of thin films of PEO/PMMA blends [43]. We first discuss some important aspects of dendritic crystallization in polymers and then focus on the dendrite tip shape, sidebranching, growth envelope, and coarsening processes in these materials. Particular emphasis is placed on the role of the PMMA molar mass and composition on the dendritic growth process.

2. Experimental

Poly(ethylene oxide) and poly(methyl methacrylate) were obtained from Scientific Polymer Products and Polymer Laboratories and used as-received [47]. The molar mass and polydispersities are reported in Table 1 [48]. In this study, crystallized blend samples are referred to by the PMMA molar mass (names indicated in Table 1). The PEO and PMMA were dissolved in 1,2-dichloroethane and stirred overnight. The polymer concentration in solution was approximately 1.25% by mass and the composition of the blend was varied from 50 to 30% PEO by mass. Silicon wafers (100) were cleaned

Table 1
Molar mass and polydispersities of polymer samples used in this study

Material	M_w (g/mol)	M_w/M_n
PEO	101 200	1.04
PMMA7	6880	1.07
PMMA12	12 000	1.08
PMMA18	17 900	1.10
PMMA53	52 700	1.08
PMMA68	68 200	1.13
PMMA101	101 000	1.09

with a boiling solution of 70% by volume sulfuric acid and 30% by volume hydrogen peroxide for 2 h to create a hydrophilic surface. After cleaning, the wafers were rinsed with deionized water and blown dry with nitrogen. Before spin-coating, the wafers were rinsed with HPLC-grade 1,2-dichloroethane and spun dry. The polymer solutions were then spin-coated onto the silicon wafer. The resulting dry film thickness was approximately 120 nm, as determined using a JA Woollam spectroscopic ellipsometer. Spin-coated samples were then dried under vacuum at 60 °C for 2 h and transferred to a Linkam heating stage. The samples were heated to 80 °C for 1 min (to melt any crystals formed during drying) and crystallized at 37 °C in a Linkam hotstage under nitrogen, unless otherwise noted. An Olympus BH-2 reflected light microscope equipped with a Cohu charge-coupled device (CCD) camera was used to observe the crystal growth morphology. The image contrast was digitally enhanced to show the morphologies more clearly. A Digital Instruments Dimension Series atomic force microscope (AFM) was used in tapping mode for higher resolution observations of the dendrite tip. AFM images were captured at room temperature in air.

3. Results and discussion

3.1. Dendritic crystallization in miscible polymer blends

Fig. 1 shows the optical micrograph of a typical dendrite observed during crystallization of a 30/70 (% by mass PEO/% by mass PMMA7) blend. To understand the nature of dendrite formation in this system, it should be pointed out that PEO crystallizes while PMMA is rejected from the growth front (as is typical of crystal/amorphous polymer blends) [49]. Due to the thin film nature of the sample, it is likely that PMMA is rejected in the plane of crystal growth [50]. In addition, the χ-parameter of PEO/PMMA is near zero, so no appreciable melting point depression is expected (while the PEO and PMMA chains are chemically different, the solution can be considered as a one-component system and phase separation occurs only through crystallization of PEO). Crystallization in this system can thus be viewed as a solution growth process where the buildup of impurities at the growth front drives the breakdown of faceted crystals into dendritic morphologies due to a non-uniform supersaturation at the solid–liquid interface.

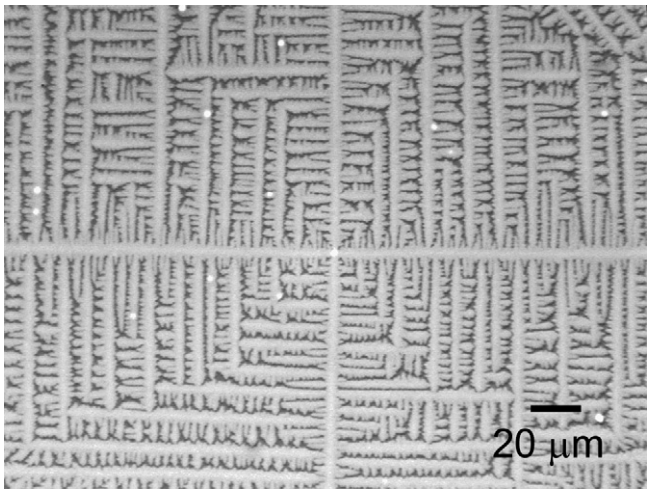

Fig. 1. Example of a dendrite in a 30/70 PMMA7 sample crystallized at 37 °C.

3.2. Dendrite tip shape

An AFM micrograph of the growth tip of a dendrite is shown in Fig. 2. The tip of the dendrite is curved and facets are apparent on either side. These dendrites have generally been called 'faceted dendrites,' in the small molecule literature [51–53]. Faceting is known to occur in small molecule systems, such as NH_4Br, under specific growth conditions and has been associated with a large anisotropy in the attachment kinetics as is expected for materials with large entropies of fusion (such as polymers).

Using the method described by Cadirli and coworkers [54], the tip radius was determined to be on the order of 50 nm (from Fig. 2). This measurement was only carried out at room temperature but was relatively independent of PMMA molar mass (there is considerable uncertainty in this measurement given the difficulty in resolving tips of such a small radius during in situ AFM experiments). The diffusion coefficient can also be estimated using the value of the tip radius and the sidebranch spacing. The sidebranch spacing near the dendrite tip is often approximated as [55]

$$\lambda \approx c_1 \sqrt{d_o \ell}$$

where c_1 is a constant, d_o is the capillary length, and ℓ is the diffusion length. The diffusion length is defined by the ratio of the diffusion coefficient (D) of the non-crystallizing species and the crystal growth rate (G):

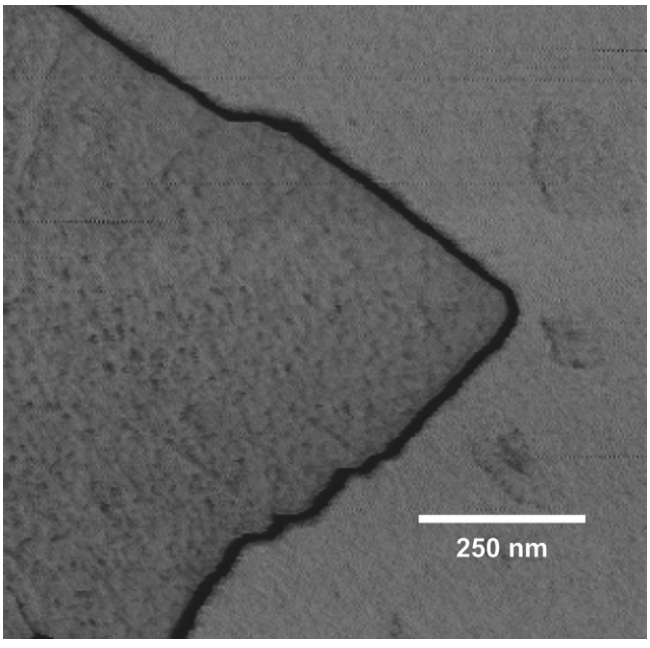

Fig. 2. Atomic force phase micrograph of a growth tip in a 30/70 PMMA68 sample growing at 25 °C.

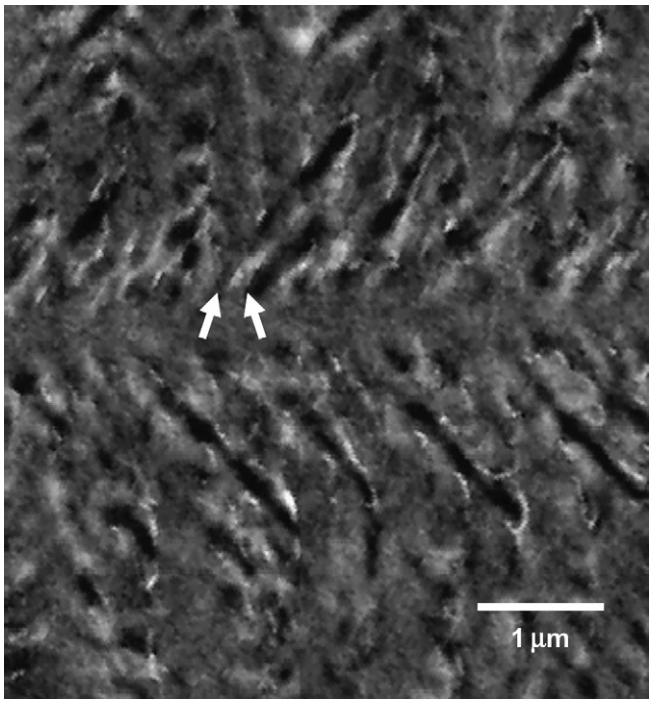

Fig. 3. Atomic force micrograph of the sidebranching near the trunk of a 30/70 PMMA18 dendrite crystallized at 37 °C. The arrows show the approximate width of one sidebranch.

$$\ell = D/G$$

Using values of $c_1 = 2.5$, $\lambda = 50$ nm, $d_o = 10^{-10}$ m, and G of 10^{-4} μm/s, the diffusion coefficient is found to be on the order of 10^{-12} cm^2/s. This estimate seems reasonable based on typical polymer diffusion coefficients [56] and measurements of the mutual diffusion coefficient in PEO/PMMA blends by Wang et al. [57], although no such measurements have been reported to date for these blends in thin films for the molar masses and crystallization temperatures used in this study. We also point out that the value of the capillary length is unknown in polymeric materials, but the typical length scale is expected to be on the order of segmental dimensions (1–10 Å) [58].

3.3. Sidebranching

As seen in Fig. 1, sidebranches appear at 90° to the dendrite trunk, reflecting the symmetry of the PEO unit cell [59]. However, inspection by atomic force microscopy reveals that these branches initially form at an angle of near 45° and turn back toward the preferred 90° direction (Fig. 3). This ''steering effect'' toward the crystallographically preferred directions has been reported in studies on small molecule dendrites [15].

Fig. 1 also reveals that the sidebranches are not well correlated along the length of the dendrite trunk. Imperfect correlation of the sidebranches has been suggested to result from the presence of noise near the dendrite tip [60–62]. Another

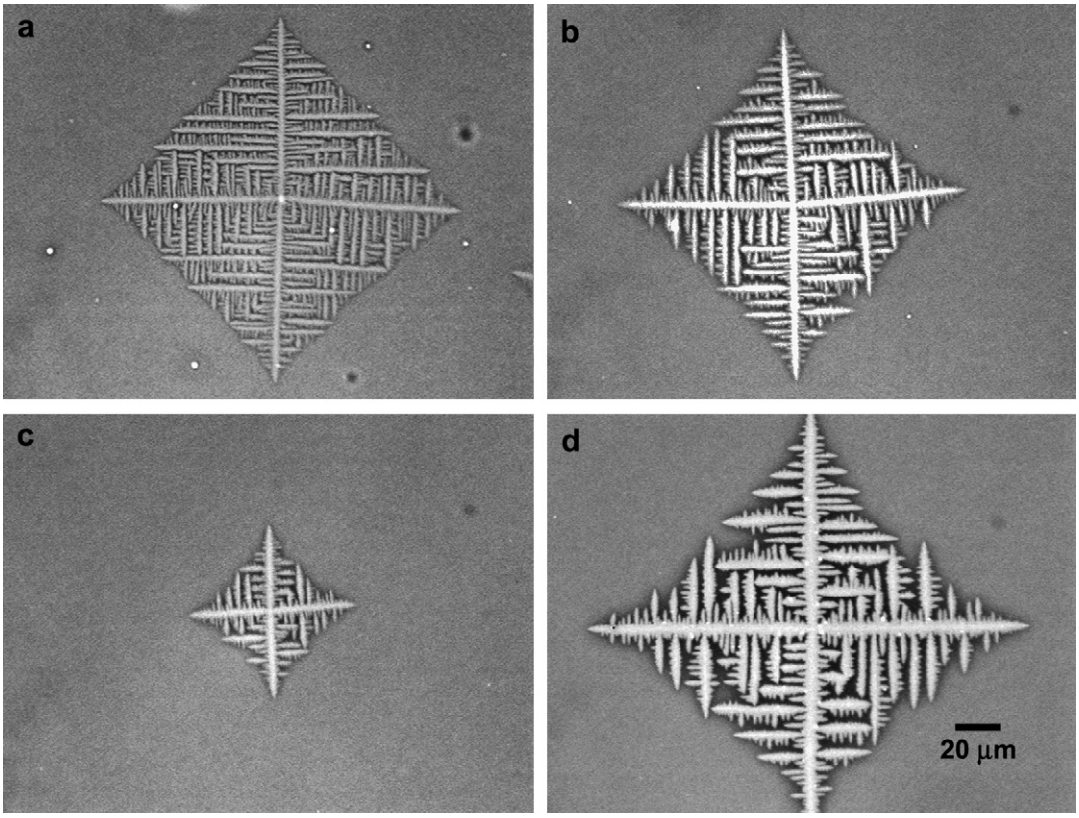

Fig. 4. Effects of the PMMA molar mass on the observed morphology for 35/65 blends crystallized at 37 °C: (a) PMMA7, (b) PMMA18, (c) PMMA68, and (d) PMMA101.

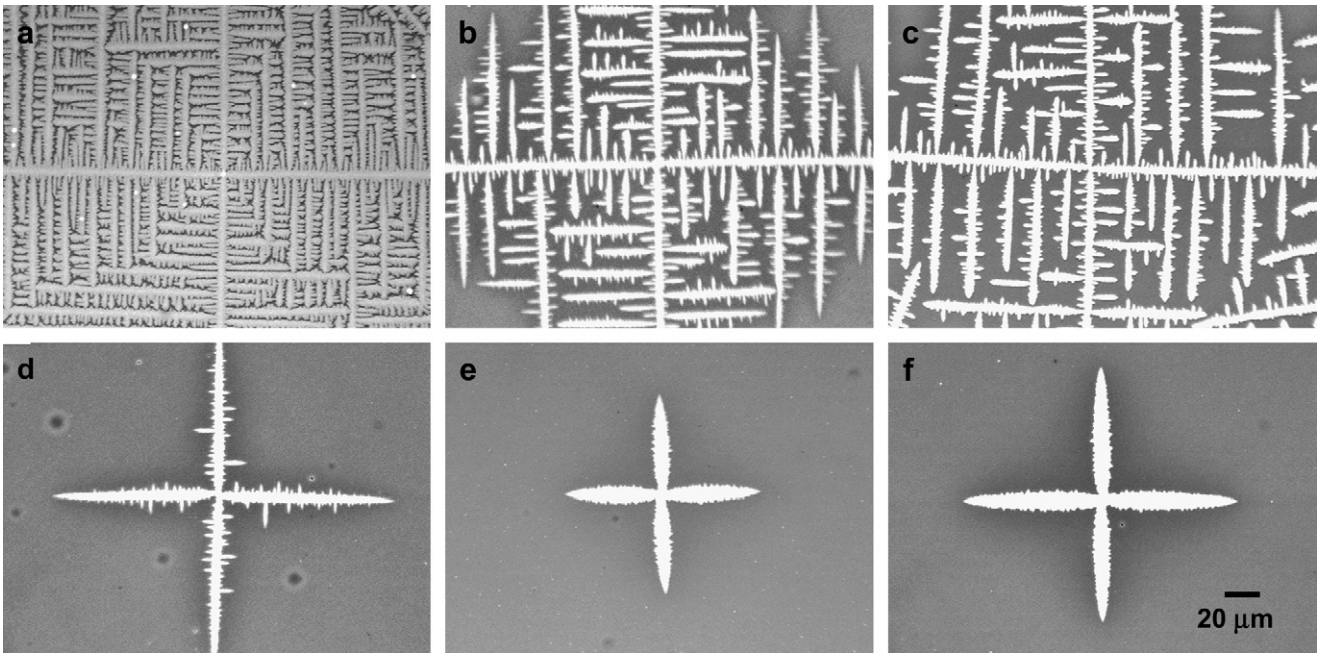

Fig. 5. Effects of the PMMA molar mass on the observed morphology for 30/70 blends crystallized at 37 °C: (a) PMMA7, (b) PMMA12, (c) PMMA18, (d) PMMA53, (e) PMMA68, and (f) PMMA101.

mechanism for sidebranch formation involves the existence of a limit-cycle during crystal growth where the growth tip slows and fattens before emitting two synchronized sidebranches [2,63,64]. Crystal growth rate measurements suggest that noise is a source of sidebranching in this system, although Ferreiro and coworkers have previously reported clear evidence for this type of oscillatory growth in PEO/PMMA blends above a critical thickness value [42]. The source of the discrepancy has not been identified, but may be related to differences in sample preparation.

In typical dendritic growth, sidebranches form about 1–5 tip radii from the growth tip [65–67]. Here, the tip radius is on the order of 50 nm (Fig. 2), so sidebranching is expected to occur at distances of 50–250 nm from the dendrite tip. The observed spacing in Fig. 3 establishes that this approximation is indeed justified for these materials.

3.4. Tuning of the diffusion coefficient and the growth envelope

As discussed above, the diffusion coefficient of polymer mixtures can be varied in a number of ways, such as varying the molar mass or the concentration of the non-crystallizable component. While a theoretical understanding of the relationship between the mutual diffusion coefficient for chains in the mixture and the self-diffusion coefficients of the individual chains is not complete [68–71], one expects the mutual diffusion coefficient to decrease with an increase in the concentration of the high glass transition temperature component or molar mass of the impurity.

In the present case, the molecular diffusion coefficient is believed to play a dominant role in the magnitude of the diffusion length. In PEO/PMMA mixtures, for example, increasing the PMMA molar mass or concentration lowers the diffusion coefficient but does not significantly affect the crystal growth rate (less than an order of magnitude for each blend composition) [72]. It should also be pointed out that these length scales are significantly smaller than those in small molecules. In small molecule systems, diffusion lengths are typically on the order of micrometers to millimeters for solute diffusion, while in high molar mass bulk polymer melts, the diffusion lengths are typically on the order of 10^{-8} to 10^{-4} cm [56]. Confinement of polymer chains into a thin film geometry and dilution of the crystallizable chains by a non-crystallizable component are expected to decrease these values significantly [73].

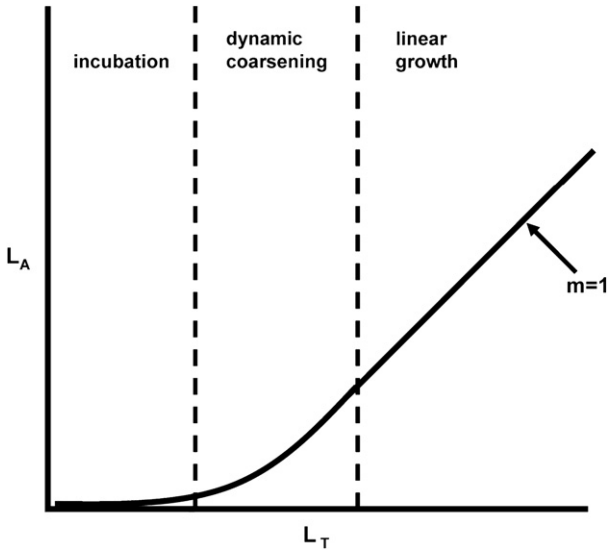

Fig. 6. Schematic of different growth regions for secondary sidebranches.

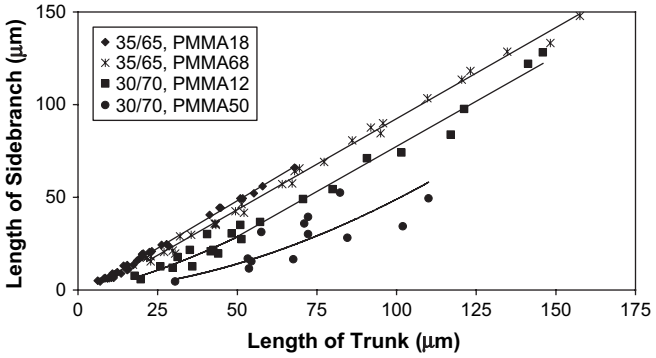

Fig. 7. Experimental values of L_A and L_T for several blends crystallized at 37 °C. The error bars are smaller than the data points.

Figs. 4 and 5 demonstrate the effects of changes in the diffusion coefficient on pattern formation through changes in the molar mass and concentration of PMMA. These changes in the diffusion coefficient become apparent when the growth envelope is examined. The growth envelope is composed of the leading dendrite tip and the train of sidebranches emanating from the trunk and contains important information about the processes involved in pattern formation, such as competition between sidebranches [74]. In cubic materials, the growth envelope takes the shape of a square diamond with concave edges that indicate the level of competition between sidebranches during growth.

Several methods are available for categorizing the shape of the crystallization envelope. We chose to measure the length of the leading dendrite arms (L_A) as a function of the distance from the dendrite tip (L_T) at a fixed time. Isothermal coarsening effects are ignored for reasons discussed later. Initially, an incubation time is observed and is associated with the stage where competition between branches sets in. Following this incubation period, the competitive growth regime begins. In this stage, the growth rate is non-linear due to competition between the diffusion fields of neighboring sidebranches. Near the dendrite tip, the length of the arms is predicted to grow as $|z|^{1/2}$, where z is the distance from the dendrite tip [1]. Once the diffusion fields begin to interact, the sidebranches are predicted to grow as $|z|^{3/5}$ [75]. The diffusion fields of the arms interact and growth is slow until 'winning' sidebranches are selected. After selection of the winning branches, these branches speed up until they have the same growth rate as the dendrite tip. These regimes are summarized in Fig. 6. If selection of the winning sidebranches takes a long time (during which the growth rate of the sidebranches is slower than that of the trunk) a concave shape is developed. For shorter selection times, the angle between the dendrite trunk and the tangent to the growth envelope rapidly nears 45°.

Experimental data for L_A versus L_T for several PMMA molar masses and blend compositions are reported in Fig. 7. For blends with a composition of 35/65, square dendrites are observed at low molar mass (see Fig. 4), indicating that the selection time for winning sidebranches is very small, and the corresponding L_A–L_T plot has a slope of 1. Increasing the PMMA content and/or molar mass drastically increases the coarsening regime and leads to a slower approach to the linear growth regime. Dendrites formed under these conditions have a needle-like shape and short sidebranches, even after long crystallization times.

These observations suggest that ''noise'' plays an important role in the selection of the winning sidebranches [76]. In the present case, ''noise'' refers to concentration or temperature fluctuations. High PMMA content or molar mass results in slower dynamics and consequently a lower level of noise, implying that growth must occur for a longer period of time before the system can reach a steady-state and winning sidebranches are selected (see for example, the dendrite in Fig. 5f where sidebranches have approximately the same length even at different distances from the dendrite tip). Fig. 8 shows the results for a phase-field model of the effects of the amplitude of thermal noise on dendritic branching. Assuming that the rate of molecular attachment is governed by diffusion, we expect that the noise parameter scales in rough proportion to the molecular diffusion coefficient ($\alpha \sim D$). As in the experiments (Fig. 5), lower noise results in less pronounced branching from the dendrite trunk.

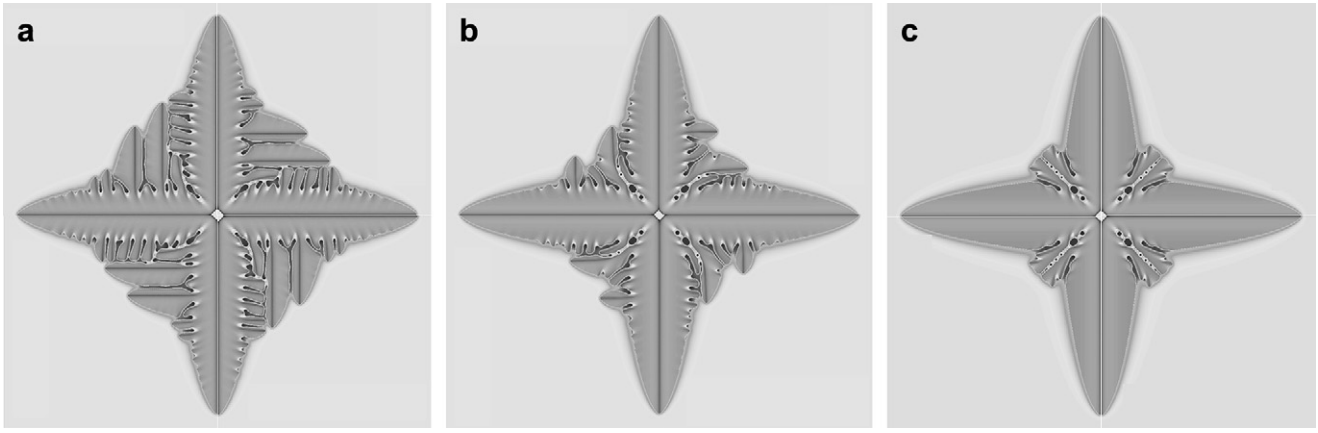

Fig. 8. Phase-field calculation of a model nickel–copper alloy showing the effects of noise on dendrite sidebranch formation. The noise amplitude in the model is varied from 0.075, 0.01875, to 0 in (a)–(c). For details of the phase-field calculation, see Ref. [77].

3.5. Dendrite coarsening

Following the initial development of sidebranches, dendrites often undergo a 'coarsening' process. Two types of coarsening processes are known to occur. One type is 'isothermal coarsening,' which involves lowering the surface energy of the crystal by reducing the crystal's surface area. This is a relatively slow process where some of the small arms disappear or merge with larger arms. The second type of coarsening process is called 'dynamic coarsening.' In this process, the secondary sidebranches continually adjust their spacing due to competition between neighboring sidebranches.

In contrast to studies on dendrites in small molecules, the sidebranch spacing in the PEO/PMMA system does not change with time at a fixed position from the dendrite trunk. That is, no isothermal coarsening is found at any observable length scale. This observation can be rationalized as follows. During crystallization, PMMA is rejected from the crystal front, resulting in an enrichment of PMMA between sidebranches. This increase in PMMA concentration raises the local glass transition temperature, effectively slowing down diffusion and hindering crystallization by limiting access to any crystallizable PEO chains. Since all branches formed during growth are still present, the sidebranch spacing can be easily analyzed after the crystallization is complete. The sidebranch spacing (S) is reported as a function of the distance from the dendrite trunk in Fig. 9. As the PMMA molar mass increases, the distance between sidebranches also increases. In our system, we also note that changes in composition have a similar effect as changes in the PMMA molar mass (see Figs. 4 and 5).

As discussed above, as the sidebranches grow, they begin to compete with each other. The slowing down of a sidebranch, as a result of competition or thermal fluctuations, may allow neighboring branches to take over and readjust their spacing. The result of this dynamic coarsening process is that the sidebranch spacing increases with distance from the dendrite trunk (or the tip). Huang and Glicksman have suggested that this competition should only occur if the diffusion fields overlap, and thus should cease when proper spacing is reached. We observe another coarsening mechanism where impingement between a sidebranch and a higher-order sidebranch growing in an orthogonal direction changes the secondary sidebranch spacing. Fig. 10 provides an example of the cutting off of a secondary sidebranch by a tertiary sidebranch originating from a neighboring secondary sidebranch (see arrows). This mechanism is particularly effective when the sidebranches develop near the tip and do not compete with neighboring sidebranches for long periods of time (they grow at the same rate as the dendrite tip). In this coarsening mechanism, the secondary sidebranch spacing *always* increases and the growth envelope is made up of increasingly higher-order sidebranches.

The sidebranch spacing as a function of solidification time is reported in Fig. 11. In this case, the 'solidification time' refers to the time in which a particular sidebranch has been growing. At a value of $S/S_{TIP} = 1$, where S_{TIP} is the sidebranch spacing near the dendrite tip, an ''incubation time'' can be defined, within which dynamic coarsening does not occur. Here, we assume a constant value of 50 nm for the sidebranch spacing near the dendrite tip based on AFM measurements described above (see Figs. 2 and 3). The incubation time is found by extrapolation of the data in Fig. 11 and the corresponding ''incubation length'' is calculated by multiplying the incubation length by the dendrite growth velocity. The incubation lengths calculated from Fig. 11 are in the nanometer range ($\approx$5 nm). These measurements were only carried out for three of the blends where a relatively large number of sidebranches were present. Although the accuracy is greatly affected by extrapolation to very small length scales using optical measurements and the assumption of a constant initial sidebranch spacing, this result is consistent with the fact that nearly square dendrites are observed (where the incubation length is expected to be small). Samples still undergoing dynamic coarsening (e.g., 30/70, PMMA68) were not studied here because of the relatively small number of measurable sidebranches (on reasonable time scales).

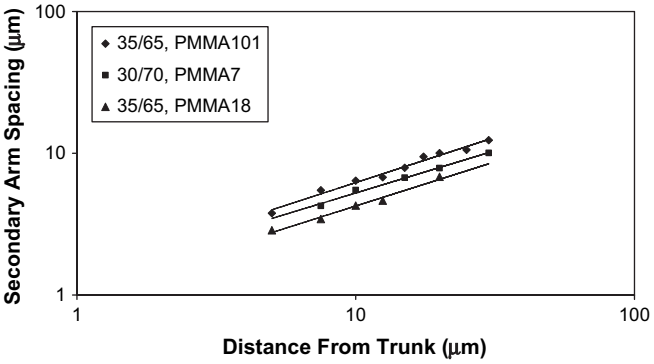

Fig. 9. Log–log plot of the secondary sidebranch spacing as a function of the distance from the dendrite trunk for several blends. The error bars are smaller than the data points.

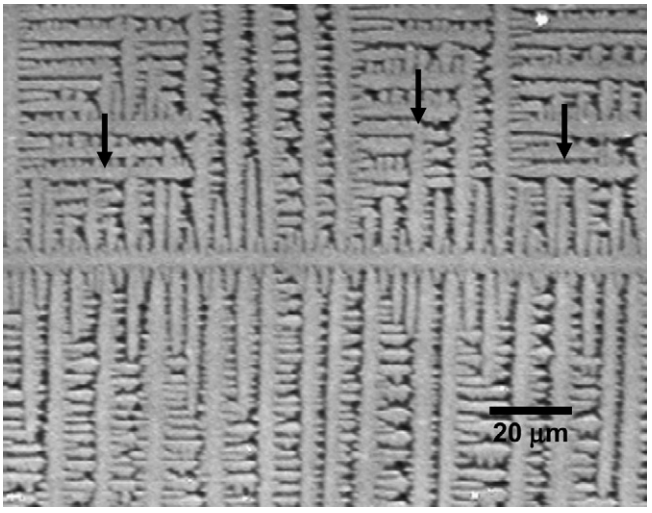

Fig. 10. Example of coarsening of the secondary sidebranch spacing by higher-order arms in a 30/70 PMMA7 blend at 33 °C. The dendrite grew from left to right.

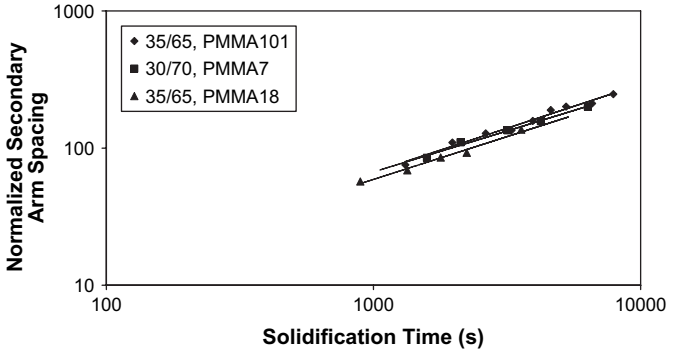

Fig. 11. The normalized secondary arm spacing as a function of solidification time for several blends. The error bars are smaller than the data points.

4. Conclusions

Dendritic crystallization of PEO/PMMA thin films is reported as a function of PMMA molar mass and concentration. The results are analyzed in the manner of Huang and Glicksman's study of small molecule dendrites and we find results quite similar to those reported in other non-polymeric systems, suggesting that the formation of dendrites in PEO/PMMA films occurs by processes similar to these systems. The radius of the growth tip was determined to be $\approx$50 nm. The sidebranch spacing was within 1–5 times the radius of curvature, which is consistent with observations in small molecule systems. The sidebranches were not correlated along the dendrite trunk, suggesting that noise is important for sidebranch formation in the present study. The role of the diffusion coefficient on pattern formation was also investigated by varying the molar mass or concentration of the non-crystallizable additive. A smaller impurity diffusion coefficient resulted in needle-like dendrites, while a larger diffusion coefficient resulted in square dendrites. These results produced trends similar to phase-field simulations where the thermal noise strength was systematically varied. As expected, the results for higher PMMA molar mass were consistent with a reduction in the effective noise strength. Coarsening of these polymer dendrites was also described in detail. Isothermal coarsening was not observed in these experiments and dynamic coarsening was only observed for high impurity concentrations and molar mass.

Acknowledgments

The authors would like to thank James Warren for the simulation images illustrating the effects of noise on dendritic growth (Fig. 8) and helpful advice. They also thank Alexander Chernov for a helpful discussion regarding crystallization in polymer mixtures.

References

[1] Dougherty A, Gunawardana A. Phys Rev E 1994;50(2):1349.
[2] Honjo H, Ohta S, Sawada Y. Phys Rev Lett 1985;55(8):841.
[3] Shibkov AA, Zheltov MA, Korolev AA, Kazakov AA, Leonov AA. J Cryst Growth 2005;285(1–2):215.
[4] Koo KK, Ananth R, Gill WN. Phys Rev A 1991;44(6):3782.
[5] Tirmizi SH, Gill WN. J Cryst Growth 1989;96(2):277.
[6] Bisang U, Bilgram JH. Phys Rev E 1996;54(5):5309.
[7] Singer HM, Bilgram JH. Phys Rev E 2004;70(3):031601.
[8] Singer HM, Bilgram JH. J Cryst Growth 2005;275:e243.
[9] Rubinstein ER, Glicksman ME. J Cryst Growth 1991;112(1):97.
[10] Honjo H, Sawada Y. J Cryst Growth 1982;58(2):297.
[11] Lee K, Losert W. J Cryst Growth 2004;269(2–4):592.
[12] Lamelas FJ, Seader S, Zunic M, Sloane CV, Xiong M. Phys Rev B 2003;67(4):045414.
[13] Glicksman ME, Schaefer RJ, Ayers JD. Metall Trans A 1976;7(11):1747.
[14] Huang SC, Glicksman ME. Acta Metall 1981;29(5):701.
[15] Huang SC, Glicksman ME. Acta Metall 1981;29(5):717.
[16] Ivanstov GP. Dokl Akad Nauk SSSR 1947;58:567.
[17] Temkin DE. Dokl Akad Nauk SSSR 1960;132:1307.
[18] Bolling GF, Tiller WA. J Appl Phys 1961;32(12):2587.
[19] Langer JS, Muller-Krumbhaar H. Acta Metall 1978;26(11):1681.
[20] Langer JS. Rev Mod Phys 1980;52(1):1.
[21] Kessler DA, Koplik J, Levine H. Adv Phys 1988;37(3):255.
[22] Glicksman ME, Marsh SP. Handbook of crystal growth. In: Fundamentals: transport and stability, vol. 1B. New York: Elsevier Science Publishers B.V.; 1993. p. 1075–122.
[23] Billia B, Trivedi R. Handbook of crystal growth. In: Fundamentals: transport and stability, vol. 1B. New York: Elsevier Science Publishers B.V.; 1993. p. 899–1073.
[24] Keith HD, Padden FJ. J Appl Phys 1963;34(8):2409.
[25] Keith HD, Padden FJ. J Appl Phys 1964;35(4):1286.
[26] Magill JH. J Mater Sci 2001;36(13):3143.
[27] Granasy L, Pusztai T, Borzsonyi T, Warren JA, Douglas JF. Nat Mater 2004;3(9):645–50.
[28] Granasy L, Pusztai T, Tegze G, Warren JA, Douglas JF. Phys Rev E 2005;72(1):011605.
[29] Keller A. Philos Mag 1957;2:1171.
[30] Khoury F, Padden FJ. J Polym Sci 1960;XLVII:455.
[31] Geil PH, Reneker DH. J Polym Sci 1961;51:569.
[32] Wunderlich B, Sullivan P. J Polym Sci 1962;61:195.
[33] Zhang F, Liu J, Huang H, Du B, He T. Eur Phys J E 2002;8(3):289.
[34] Taguchi K, Miyaji H, Izumi K, Hoshino A, Miyamoto Y, Kokawa R. Polymer 2001;42(17):7443.
[35] Beers KL, Douglas JF, Amis EJ, Karim A. Langmuir 2003;19(9):3935.
[36] Taguchi K, Toda A, Miyamoto Y. J Macromol Sci Phys 2006;45:1141.
[37] Zhai X, Wang W, Zhang G, He B. Macromolecules 2006;39(1):324.
[38] Mareau VH, Prud'homme RE. Macromolecules 2005;38(2):398.
[39] Mareau VH, Prud'homme RE. Polymer 2005;46:7255.
[40] Reiter G, Botiz I, Graveleau L, Grozev N, Albrecht K, Mourran A, et al. Progress in understanding of polymer crystallization. New York: Springer-Verlag; 2007. p. 179–200.
[41] Ferreiro V, Douglas JF, Warren JA, Karim A. Phys Rev E 2002; 65(4):042802.
[42] Ferreiro V, Douglas JF, Warren J, Karim A. Phys Rev E 2002; 65(5):051606.
[43] Okerberg BC, Marand H. J Mater Sci 2007;42(12):4521.
[44] Xu HJ, Matkar R, Kyu T. Phys Rev E 2005;72(1):011804.
[45] Toth Katona T, Borzsonyi T, Varadi Z, Szabon J, Buka A, Gonzalez-Cinca R, et al. Phys Rev E 1996;54(2):1574.
[46] Akamatsu S, Bouloussa O, To KW, Rondelez F. Phys Rev A 1992;46(8):R4504.
[47] Certain equipment, instruments, or materials are identified in this paper in order to adequately specify the experimental details. Such identification does not imply recommendation by the National Institute of Standards and Technology nor does it imply that the materials are necessarily the best available for the purpose.
[48] According to ISO 31-8, the term "molecular weight" has been replaced by "relative molecular mass," symbol M_r. The conventional notation, rather than the ISO notation, has been employed for this publication.
[49] Russell TP, Ito H, Wignall GD. Macromolecules 1988;21(6):1703.
[50] Keith HD, Padden FJ. J Polym Sci Part B Polym Phys 1987;25(11):2371.
[51] Maurer J, Bouissou P, Perrin B, Tabeling P. Europhys Lett 1989;8(1):67.

[52] Benamar M, Pomeau Y. Europhys Lett 1988;6(7):609.
[53] Adda Bedia M, Ben Amar M. Growth and form. New York: Plenum Press; 1991. p. 187.
[54] Cadirli E, Karaca I, Kaya H, Marasli N. J Cryst Growth 2003;255(1–2): 190.
[55] Muller-Krumbhaar H, Zimmer M, Ihle T, Saito Y. Physica A 1996; 224(1–2):322.
[56] Schultz JM. Polymer 1991;32(18):3268.
[57] Wang CH, Zhang XQ, Fytas G, Kanetakis J. J Chem Phys 1989;91(5): 3160.
[58] Langer JS. Science 1989;243(4895):1150.
[59] Kovacs AJ, Lotz B, Keller A. J Macromol Sci Phys 1969;B3:385.
[60] Pieters R, Langer JS. Phys Rev Lett 1986;56(18)):1948.
[61] Kessler DA, Levine H. Europhys Lett 1987;4(2):215.
[62] Bouissou P, Chiffaudel A, Perrin B, Tabeling P. Europhys Lett 1990; 13(1):89.
[63] Morris LR, Winegard WC. J Cryst Growth 1967;1:245.
[64] Sawada Y, Perrin B, Tabeling P, Bouissou P. Phys Rev A 1991;43(10):5537.
[65] Dougherty A, Gollub JP. Phys Rev A 1988;38(6):3043.
[66] Van der Eerden JP, Muller-Krumbhaar H. Acta Metall 1986;34(5):839.
[67] Vandriel CA, Van der Heijden AEDM, Van Rosmalen GM. J Cryst Growth 1993;128(1–4):229.
[68] Brochard F, Jouffroy J, Levinson P. Macromolecules 1984;17(12): 2925.
[69] Kramer EJ, Green P, Palmstrom CJ. Polymer 1984;25(4):473.
[70] Sillescu H. Makromol Chem Rapid Commun 1984;5(9):519.
[71] Shearmur TE, Clough AS, Drew DW, van der Grinten MGD, Jones RAL. Macromolecules 1996;29(22):7269.
[72] Alfonso and Russell (Alfonso G, Russell TP. Macromolecules 1986;19:1143.) showed a weaker dependence of the crystal growth rate on the PMMA content at high PMMA content. For the narrow range of blend compositions studied here, the compositional dependence of the growth rate should be small.
[73] Lin EK, Wu W, Satija SK. Macromolecules 1997;30(23):7224.
[74] Sakaguchi H, Ohtaki M. Physica A 1999;272(3–4):300.
[75] Brener E. Phys Rev Lett 1993;71(22):3653.
[76] Kobayashi R. Physica D 1993;63:410.
[77] Warren JA, Boettinger WJ. Acta Metall Mater 1995;43(2):689.